 https://doi.org/10.5812/jrps-159451

Published Online: 2025 August 11

Research Article

Natural Marine-derived Compounds as Potential Inhibitors of SARS-CoV-2 Main Protease: A Comprehensive Computational Study

Ghazal Nowroozi [1], Shokoufeh Rahmani [1], Parvin Jalali [1], Armin Zareie [1], Zahra Asvar [2, *], Amin Nowroozi [3, **]

[1] Nano Drug Delivery Research Center, Health Technology Institute, Kermanshah University of Medical Sciences, Kermanshah, Iran
[2] Fertility and Infertility Research Center, Health Technology Institute, Kermanshah University of Medical Sciences, Kermanshah, Iran
[3] Pharmaceutical Sciences Research Center, Health Institute, Kermanshah University of Medical Sciences, Kermanshah, Iran

[*] ***Corresponding Author:*** Fertility and Infertility Research Center, Health Technology Institute, Kermanshah University of Medical Sciences, Kermanshah, Iran. Email: z_asvar@yahoo.com
[**] ***Corresponding Author:*** Department of Medicinal Chemistry, Faculty of Pharmacy, Kermanshah University of Medical Sciences, Kermanshah, Iran. Email: amin.nowroozi@yahoo.com

Received: 18 February, 2025; **Revised:** 18 May, 2025; **Accepted:** 22 May, 2025

Abstract

Background: The COVID-19 pandemic, caused by the SARS-CoV-2 virus, highlights the urgent need for effective antiviral agents. The main protease [3-chymotrypsin-like protease (3CLpro)] of SARS-CoV-2 is crucial for viral replication and is a promising target for therapeutic intervention.

Objectives: In this study, an in silico approach was employed to identify potential 3CLpro inhibitors from a library of 80 marine-derived natural compounds.

Methods: Molecular docking was performed using AutoDock Vina to assess the binding affinity and interaction profiles of the compounds with the active site of 3CLpro. The top-scoring compounds were selected for molecular dynamics simulations using GROMACS to analyze the structural stability and dynamic behavior of the ligand-protease complexes.

Results: Several compounds, particularly those from marine fungi and sponges, formed stable interactions with catalytic residues His41 and Cys145, maintaining conformational stability throughout 100 ns of simulation. In silico ADMET assessments were further performed to predict the pharmacokinetic properties of the docked compounds. Overall, molecular dynamics (MD) analysis showed that the dynamic properties of the protein alter significantly when it is in complex with the selected compounds.

Conclusions: The findings in this study suggest that Isobutyrolactone II and Aspernolide A, marine natural products, could serve as promising lead compounds for the development of SARS-CoV-2 main protease inhibitors, warranting further experimental validation.

Keywords: Marine Natural Products, SARS-CoV-2, 3CLpro, Molecular Docking, Molecular Dynamics Simulations

1. Background

RNA viruses are a diverse group of human pathogens capable of triggering rapid seasonal outbreaks, posing serious public health challenges. COVID-19, caused by SARS-CoV-2, has recently evolved into a global pandemic with millions of deaths (1-3). Although primarily a respiratory illness, the disease also leads to various extrapulmonary complications due to the widespread presence of angiotensin-converting enzyme 2 (ACE2) receptors in different organs. These include thrombotic events, hyperglycemia, cardiac arrhythmias, acute coronary syndromes, kidney injury, gastrointestinal and liver dysfunctions, as well as neurological, ocular, and dermatological symptoms (4).

SARS-CoV-2 has a large positive-sense RNA genome comprising 14 open reading frames (ORFs). The 5′ ORFs (orf1a and orf1ab) encode polyproteins pp1a and pp1ab, which are cleaved into 16 nonstructural proteins (nsp1 - 16), while the 3′ region encodes structural proteins:

How to Cite: Nowroozi G, Rahmani S, Jalali P, Zareie A, Asvar Z, et al. Natural Marine-derived Compounds as Potential Inhibitors of SARS-CoV-2 Main Protease: A Comprehensive Computational Study. J Rep Pharm Sci. 2025; 13 (1): e159451. https://doi.org/10.5812/jrps-159451.

Spike (S), envelope (E), membrane (M), and nucleocapsid (N) (5). Proteolytic cleavage of the polyproteins is catalyzed by two key enzymes: Three-chymotrypsin-like protease (3CLpro) and papain-like protease (PLpro) (6). Among them, 3CLpro, the main protease, consists of three domains — β-barrel domains I and II, and α-helical domain III — with the catalytic dyad HIS41 and CYS145 located between domains I and II (7).

Given the unique catalytic mechanism of 3CLpro, distinct from human proteases, its inhibition can effectively block viral replication, offering a promising target for specific antiviral therapies (8). Importantly, the high conservation of viral protease active sites reduces the likelihood of resistance development compared to vaccines (9). Although traditional drug discovery is often slow and expensive, natural compounds — especially those amenable to large-scale production — are gaining attention for their antiviral potential (10).

Marine organisms, which inhabit the majority of Earth's surface, produce diverse secondary metabolites in response to environmental stressors. These compounds possess distinctive structural and functional characteristics, setting them apart from terrestrial natural products, and have shown promising antiviral activities. Given the rapid mutation and global spread of SARS-CoV-2, marine-derived agents represent a valuable resource for novel antiviral development (11).

Drug discovery is inherently complex, requiring interdisciplinary strategies to enhance efficiency and reduce cost. In this context, computational tools such as molecular docking and molecular dynamics (MD) simulations play a crucial role. Molecular docking predicts the interaction modes and affinities of small molecules with target proteins, while MD simulations provide insights into the dynamic behavior and conformational changes of protein-ligand complexes over time (12-14).

2. Objectives

In this study, we utilize these computational tools to explore the interactions between marine-derived compounds and the SARS-CoV-2 3CLpro protease. Through molecular docking and subsequent MD simulations, we identify promising inhibitors that may be developed into effective antiviral agents. The pharmacological properties of the most promising compounds are also evaluated to guide future experimental research.

3. Methods

3.1. Preparation of the Receptor and Ligands

The three-dimensional (3D) crystal structure of the SARS-CoV-2 main protease (3CLpro) was retrieved from the RCSB Protein Data Bank (PDB; ID: 7BAJ). The chemical structures of the selected marine-derived compounds (15, 16) were first sketched in two-dimensional (2D) format using the ACD/Labs software. These structures were then converted into 3D conformations and subjected to energy minimization using the steepest descent algorithm in the Avogadro software.

3.2. Molecular Docking Studies

Molecular docking was employed to predict the binding affinity and orientation of ligands within the active site of 3CLpro (17, 18). Docking simulations were performed using AutoDock Vina. Prior to docking, all ligand torsions were set as rotatable, and receptor preparation, including the addition of polar hydrogens, assignment of Gasteiger charges, and atom typing according to the AutoDock force field, was carried out using MGLTools. The docking grid was centered on the protease's catalytic dyad (His41 and Cys145), defining the active site. Each of the 80 marine compounds was subjected to 20 docking runs. Ligands exhibiting binding energies lower than -7 kcal/mol (Table 1) and interacting with the active site residues were selected for further evaluation of pharmacokinetic properties and drug-likeness using the SwissADME web server (http://www.swissadme.ch). Based on these assessments, five promising candidates with proper interaction energies and pharmacokinetic properties were chosen for MD simulations.

3.3. Molecular Dynamic Simulation

The MD simulations were performed using the GROMACS 2018 package (19) to assess the structural stability and dynamic behavior of five ligand-3CLpro complexes. Ligand topologies were prepared via the Antechamber software, and the protein topology was generated using the AMBER99SB-ILDN force field (20). Each complex was solvated in a cubic box with TIP3P water molecules, and counterions were added for charge neutrality. Energy minimization was achieved through the steepest descent method until atomic forces dropped below 10 kJ/mol/nm (21). Periodic boundary conditions were applied in all spatial dimensions, and equilibration was performed under both NVT and NPT ensembles at 310 K and 1 bar using the V-rescale thermostat (22) and Martonak et al. (23), respectively. Short-range electrostatic and van der Waals interactions were calculated with a 1.0 nm cutoff, and

Table 1. Binding Energies of 45 Selected Marine-derived Compounds Against SARS-CoV-2 Main Protease (3CLpro) from Molecular Docking Simulations

Compound	Lowest Binding Energy (kcal/mol)
3-methoxydebromoaplysiatoxin	-8.2
Alterporriol Q	-7.9
Arisugacin A	-7.7
Asebotin	-7.5
Aspernolide A	-7.4
Asperterrestide A	-7.4
Baculiferins k	-8.4
BaculiferinsC	-8.4
BaculiferinsE	-7.5
BaculiferinsF	-8
BaculiferinsH	-7.2
BaculiferinsL	-8.1
BaculiferinsM	-8.3
BaculiferinsN	-8.5
briacavatolides E	-7.6
Cadiolide B	-8.3
Cordyol C	-7
Diekol	-8
DurumolideJ	-7.8
Ehrenbergol C	-7
Gyrosanol A	-7.9
Halistanolsulfate	-7.3
HipostroneN	-7.4
Isobutyrolactone II	-7.4
Khayanolides	-7.2
Manoalide	-7.2
Manzamine A	-7.5
MirabamidesH	-7.4
Mollamide E	-7.1
Mollamide F	-7.5
Molleurea A	-7.1
Myticin	-7
Norlichexanthone-3,6,8-Trihydroxy-1-methylxanthone	-7.4
Nortopsentins	-7.6
Penipanoid C	-7.4
Phlorofucofuroeckol	-7.6
Polyhydroxylated steroids	-7.5
Polyhydroxylated sterol	-7.7
Prunolide A	-7.5
Quercetin-3-O-β-D-xylopyranoside	-8.6
Rubrolide S	-7.5
Sorbicatechols A	-7.2
Stachybotrins D	-7.9
ThalassiolinD	-8
Thalassodenrone	-7.4
Triterpenoids	-7.5

bond constraints were applied using the LINCS algorithm (24). Simulations were run for 100 ns using the leap-frog integrator (25). Post-simulation analyses, including structural evaluations and trajectory visualizations, were carried out using VMD, and 2D interaction diagrams were generated with LigPlot+ (26).

4. Results and Discussion

4.1. Molecular Docking Studies

Molecular docking was utilized to assess the binding affinity and orientation of 80 marine-derived natural compounds against the SARS-CoV-2 main protease (3CLpro). Compounds with binding energies below -7 kcal/mol were considered promising, resulting in the selection of 45 candidates for further pharmacokinetic

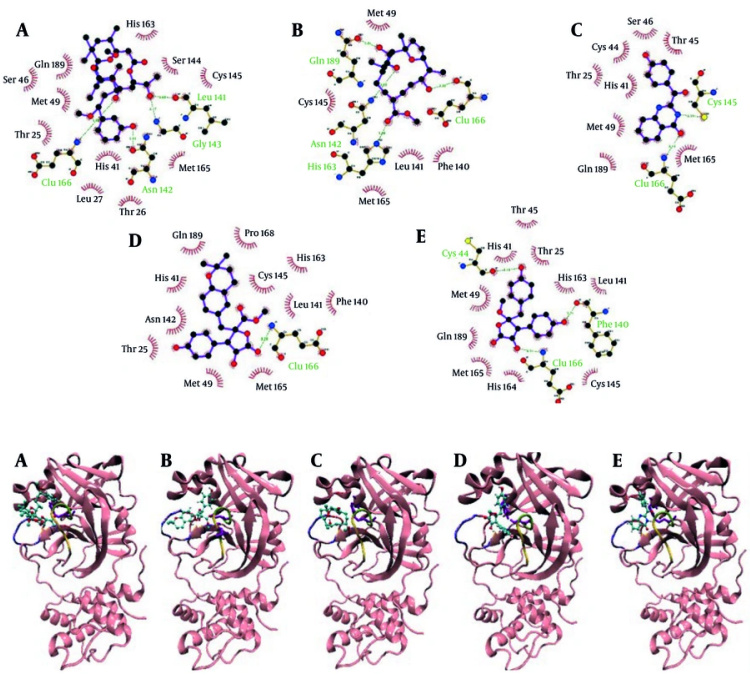

Figure 1. Two-dimensional (2D) and three-dimensional (3D) visualizations of selected marine compounds docked with the active site of SARS-CoV-2 3-chymotrypsin-like protease (3CLpro): A, 3-Methoxydebromoaplysiatoxin; B, Aspernolide A; C, Ehrenbergol C; D, Isobutyrolactone II; and E, Penipanoid C.

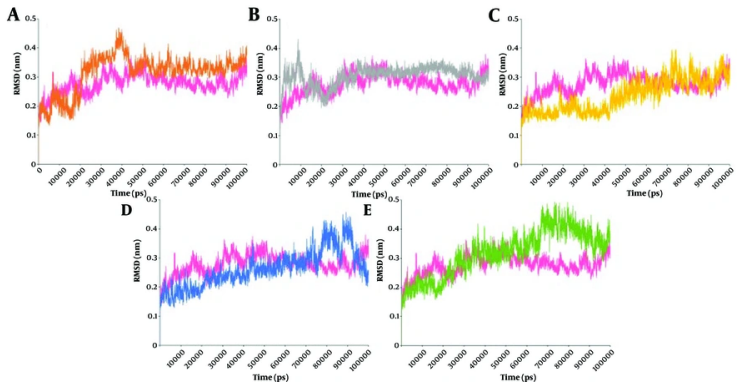

Figure 2. Root mean square deviation (RMSD) profiles over time for five protein-ligand complexes: A, 3-Methoxydebromoaplysiatoxin; B, Aspernolide A; C, Ehrenbergol C; D, Isobutyrolactone II; and E, Penipanoid C. The RMSD profile of the free protein is shown in pink for comparison.

and drug-likeness evaluation via the SwissADME server. Docking scores are listed in Table 1. Based on the docking and ADME results, five top-performing ligands (Appendices 1 and 2 in Supplementary File) — 3-methoxydebromoaplysiatoxin, Aspernolide A, Ehrenbergol C, Isobutyrolactone II, and Penipanoid C — were selected for detailed interaction analysis and subsequent molecular dynamics simulations.

Docking interaction visualization (Figure 1) revealed the detailed binding of 3-methoxydebromoaplysiatoxin to active site residues, including the catalytic dyad His41

and Cys145, through multiple hydrogen bonds and hydrophobic contacts. Aspernolide A formed critical interactions with domain I residues and Glu166, engaging the catalytic site and suggesting enzyme interference. Ehrenbergol C showed stable hydrogen bonding with residues in domains I and II, including Cys145, implying partial inhibition of substrate access. Isobutyrolactone II interacted strongly with both catalytic residues and several nearby residues, indicating potential enzymatic blockage. Penipanoid C established hydrogen and van der Waals interactions with residues essential to catalysis, possibly disrupting substrate cleavage. Overall, the docking results indicate that these marine compounds have a strong affinity for the 3CLpro active site, justifying further investigation through MD simulations.

4.2. Molecular Dynamics Simulations

Molecular dynamics simulations were performed using 100 ns all-atom trajectories to study the conformational stability and interaction patterns of selected marine-derived compounds with the SARS-CoV-2 main protease (3CLpro). Analyses included assessments of changes in binding mode and persistence (Appendix 3 in Supplementary File), interaction dynamics, and structural changes over time. For 3-Methoxydebromoaplysiatoxin, hydrogen bonds were reduced to two with Thr26 and Met49 in domain I, and the compound retained interaction only with Cys145, indicating a slight shift from its original binding pose. Aspernolide A preserved interactions with domain II residues (Met165, Val142, Arg188, Gln189) and maintained two hydrogen bonds with His41 and Glu166, although the total number of interactions declined. Ehrenbergol C lost several original contacts and retained only hydrophobic interactions with Glu166, Gln189, and Thr190 in domain II, suggesting weakened binding. Isobutyrolactone II established a strong hydrogen bond with Glu47 and retained interactions with domain I residues and the catalytic dyad His41 and Cys145, supporting its stable binding. Penipanoid C also showed reduced residue interactions post-simulation but preserved contacts with catalytic residues His41 and Cys145, formed a stable hydrogen bond with Glu166, and retained van der Waals interactions with Met49, Met165, and Gln189, indicating potential to inhibit enzymatic function. Collectively, these findings demonstrate that while marine-derived ligands undergo subtle conformational adjustments during MD simulations, they retain stable binding interactions with the active site of the protease. The persistent structural integrity of the complexes, coupled with sustained ligand-enzyme contact at the catalytic site, suggests a plausible mechanistic basis for their protease inhibitory activity.

Root mean square deviation (RMSD) analysis over 100 ns for protein backbone atoms revealed that the unbound protease initially increased in RMSD during the first 20 ns and then stabilized (Figure 2). The 3-Methoxydebromoaplysiatoxin complex showed its highest RMSD peak near 40 ns and stabilized around 0.36 nm thereafter. The Aspernolide A complex fluctuated in the first 20 ns, then stabilized around 0.33 nm, about equal to the free protein from 40 ns onward. The Isobutyrolactone II and Penipanoid C complexes both showed rising RMSD trends. Penipanoid C and Isobutyrolactone II had values exceeding 0.42 nm, especially between 70 - 100 ns, whereas Ehrenbergol C had the lowest average RMSD. These results suggest that different ligands exert distinct effects on the protease's conformational dynamics.

Figure 3 illustrates how the binding of marine-derived ligands to the 3CLpro influences residue flexibility across its domains. In the 3-Methoxydebromoaplysiatoxin-3CLpro complex, root mean square fluctuation (RMSF) decrements were observed at residues in domains I (41 - 45, 46 - 52, 59 - 70, 84), II (139 - 142, 180 - 187), and III (188 - 193). Along with increased fluctuations in residues 7 - 15, 91 - 100 (domain I), 101 - 111, 118 - 124, 128 - 137 (domain II), and 223 - 234, 236 - 258, 275 - 306 (domain III), these suggested variable changes in the flexibility of domains I and II, and increased flexibility in domain III.

For Aspernolide A, RMSF increased at residues in domains I (19 - 24, 55 - 65, 92 - 98), II (105 - 115, 116 - 134, 137 - 141, 158 - 165), and III (188 - 191, 274 - 279), while decreases occurred at residues 7 - 17, 50 - 52, 72, 76 - 87 (domain I), 177 - 183, 185 - 190 (domain II), and across most of domain III. The Ehrenbergol C complex showed RMSF decreases at residues 43 - 50, 63 - 65, 72, 83 - 86 (domain I), 140 - 142, 169 - 174, 177 - 181 (domain II), and 182 - 194, 224 - 226, 229 - 239, 252 - 263 (domain III). Increases were found at residues 106 - 116, 120 - 134, 155 (domain II) and 202 - 220, 245 - 252, 275 - 306 (domain III). Isobutyrolactone II caused increased RMSF at residues in domains I (67 - 70, 75 - 83), II (88 - 100, 102 - 116, 118 - 145, 153 - 171), and III (200 - 207, 213 - 227, 237 - 306), while decreases were noted at 46 - 50, 56, 61 - 63 (domain I), 183 - 196 (domain II), and 208 - 211 (domain III). Penipanoid C induced RMSF decreases at residues 14, 41 - 52, 54 - 59, 64 (domain I), 115, 119 - 135, 139 - 142, 168 - 182 (domain II), and 183 - 196, 209, 231 - 235 (domain III), with increases at 71, 75 - 80, 91 - 98 (domain I), 102 - 112 (domain II), and 203 - 306 (domain III). In conclusion, ligand binding significantly affects the flexibility of key regions in 3CLpro involved in catalysis

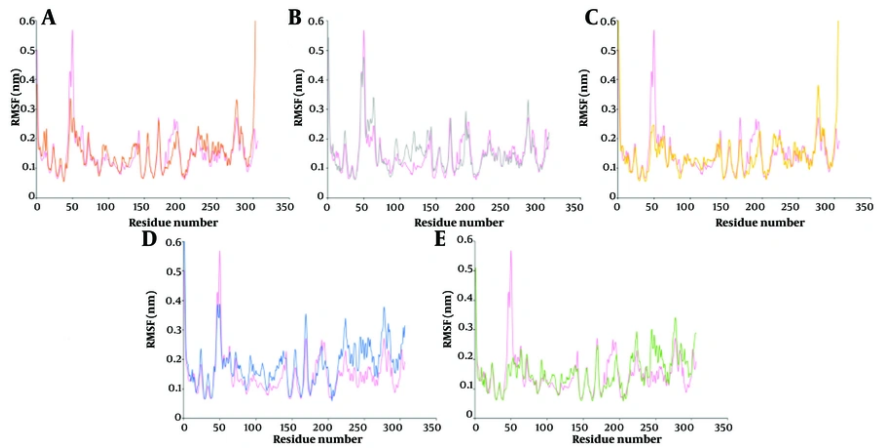

Figure 3. Root mean square fluctuation (RMSF) profiles of Cα atoms for five protein–ligand complexes: A, 3-Methoxydebromoaplysiatoxin; B, Aspernolide A; C, Ehrenbergol C; D, Isobutyrolactone II; and E, Penipanoid C. The RMSF profile of the free protein is shown in pink for comparison.

and substrate binding, supporting the inhibitory potential of these marine-derived compounds.

The radius of gyration (Rg) analysis measures the overall changes in the diameter of a protein. Changes in Rg indicate conformational variations that could affect substrate binding to the catalytic pocket. The Rg profiles of the free protein and its complexes with various marine compounds are shown in Appendix 4. The free protein showed some compactness with fluctuations around an average of 2.16 nm, showing a downward trend during the simulation. In contrast, complexes with all ligands prevent the final Rg reductions in ligand-bonded protein when compared with the free protein. The highest fluctuations were seen in complexes with Ehrenbergol C, Isobutyrolactone II, Aspernolide A, and 3-Methoxydebromoaplysiatoxin, suggesting more structural instability and potential enzyme dysfunction.

Solvent-accessible surface area (SASA) analysis, shown in Appendix 5, revealed a small increase in the SASA value in the Isobutyrolactone II complex, indicating a structural change of the protein in the presence of this ligand. As shown in the figure, in other complexes, the final SASA value is in the range of the free protein with some differences in diagram patterns. The most severe fluctuations in SASA value during the simulation are observed in the protein complex with Penipanoid C and 3-Methoxydebromoaplysiatoxin.

Principal component analysis (PCA) extracted the protein's movement patterns, as shown in Figure 4. The free protein exhibited a value range of -7 to 8 nm in PC1. All marine compounds altered the range and pattern of conformational values in PCs, indicating their potential to destabilize the structure. Notably, Penipanoid C caused the largest increase in protein mobility, consistent with the Rg results, showing significant fluctuations. In contrast, complexes with Isobutyrolactone II, Aspernolide A, and Ehrenbergol C showed reduced protein mobility, with the most severe restriction observed in Isobutyrolactone II. These findings suggest that these marine compounds could cause conformational changes and movement patterns of the protease, hindering the protein's activity.

The Define Secondary Structure of Proteins (DSSP) analysis (Appendix 6 in Supplementary File) demonstrated changes in the protein's secondary structures resulting from ligand binding. For example, 3-methoxydebromoaplysiatoxin destabilized an alpha-helix between residues 50 - 60 and removed a turn between 170 - 180. Aspernolide A disrupted beta - sheets between residues 90 - 130, while Ehrenbergol C removed a turn at residues 40 - 50. Isobutyrolactone II induced an alpha-helix formation between residues 10 - 20 and removed a turn at 40 - 50. Penipanoid C promoted alpha-helix formation at residues 10 - 20 and 50 - 60, and coils at 190 - 200. These alterations suggest that ligand binding impacts the protein's secondary structure and may affect its enzymatic activity.

Pharmacokinetic analysis of the marine compounds (Appendices 1 and 2 in Supplementary File), performed using the Swiss ADME server, revealed that all compounds exhibited good drug-likeness. Notably,

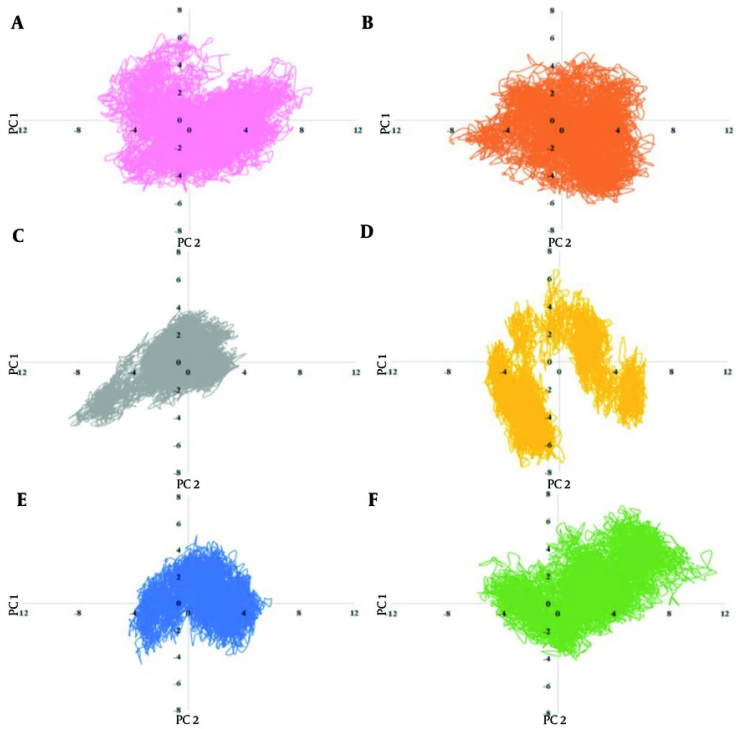

Figure 4. Principal component analysis (PCA) patterns of: A, free protein, and protein complexes with B, 3-Methoxydebromoaplysiatoxin; C, Aspernolide A; D, Ehrenbergol C; E, Isobutyrolactone II; and F, Penipanoid C.

Ehrenbergol C and Isobutyrolactone II did not interact with hepatic metabolism enzymes, suggesting a lower likelihood of drug interactions. Aspernolide A and Penipanoid C interacted with CYP2C9, CYP3A4, and CYP1A2, potentially interfering with anti-inflammatory drug metabolism. All five compounds exhibited high digestive absorption and the ability to cross the blood-brain barrier, suggesting efficient distribution and potential effectiveness in reaching viral enzymes.

4.3. Conclusions

This study computationally assessed 80 marine-derived compounds for their inhibitory potential against the SARS-CoV-2 main protease (3CLpro). Based on binding affinity and ADMET analysis, five lead compounds — 3-methoxydebromoaplysiatoxin, Aspernolide A, Ehrenbergol C, Isobutyrolactone II, and Penipanoid C — were selected for MD simulations.

The MD results showed that complexes with Isobutyrolactone II, Ehrenbergol C, and 3-methoxydebromoaplysiatoxin exhibited the highest RMSD values, with Isobutyrolactone II causing the greatest fluctuations, confirmed by both RMSD and residue-level analysis. The Rg analysis indicated notable diagram fluctuations in 3-methoxydebromoaplysiatoxin, Ehrenbergol C, and Isobutyrolactone II complexes, while others remained structurally more stable. The results of PCA revealed altered protein motion in all complexes, with the most significant limitation in protein movement observed for Isobutyrolactone II, Ehrenbergol C, and Aspernolide A, likely affecting enzymatic function. SwissADME pharmacokinetic analysis identified Isobutyrolactone II and Penipanoid C as having the most favorable pharmacokinetic profiles due to favorable absorption and metabolic characteristics. Integrative analysis of computational data nominates Isobutyrolactone II and Aspernolide A as high-priority candidates for SARS-CoV-2 antiviral development. Their persistent interaction with the viral protease active site, alongside their negative effects on the normal dynamics of the protein, underscores their inhibitory potential, necessitating

further investigation in biological systems to confirm therapeutic utility.

Supplementary Material

Supplementary material(s) is available here [To read supplementary materials, please refer to the journal website and open PDF/HTML].

Footnotes

Authors' Contribution: G. N.: Molecular modeling implementation, and original draft preparation; S. R. and P. J.: Methodology design, result analysis, and original draft writing; A. Z.: Methodology development and manuscript revision; Z. A. and A. N.: Project supervision, administration, research support, contribution to research conceptualization, methodology design, data interpretation, manuscript writing and editing.

Conflict of Interests Statement: The authors declare no conflict of interest.

Data Availability: The data supporting the findings of this study are available from the corresponding author upon reasonable request.

Funding/Support: This study was supported in part by grant 50005787 from the Kermanshah University of Medical Sciences, Kermanshah, Iran.

References

1. Guo YR, Cao QD, Hong ZS, Tan YY, Chen SD, Jin HJ, et al. The origin, transmission and clinical therapies on coronavirus disease 2019 (COVID-19) outbreak - an update on the status. *Mil Med Res*. 2020;**7**(1):11. [PubMed ID: 32169119]. [PubMed Central ID: PMC7068984]. https://doi.org/10.1186/s40779-020-00240-0.
2. Tazikeh-Lemeski E, Moradi S, Raoufi R, Shahlaei M, Janlou MAM, Zolghadri S. Targeting SARS-COV-2 non-structural protein 16: a virtual drug repurposing study. *J Biomol Struct Dyn*. 2021;**39**(13):4633-46. [PubMed ID: 32573355]. [PubMed Central ID: PMC7332864]. https://doi.org/10.1080/07391102.2020.1779133.
3. Fathollahi M, Motamedi H, Hossainpour H, Abiri R, Shahlaei M, Moradi S, et al. Designing a novel multi-epitopes pan-vaccine against SARS-CoV-2 and seasonal influenza: in silico and immunoinformatics approach. *J Biomol Struct Dyn*. 2024;**42**(20):10761-84. [PubMed ID: 37723861]. https://doi.org/10.1080/07391102.2023.2258420.
4. Gupta A, Madhavan MV, Sehgal K, Nair N, Mahajan S, Sehrawat TS, et al. Extrapulmonary manifestations of COVID-19. *Nat Med*. 2020;**26**(7):1017-32. [PubMed ID: 32651579]. [PubMed Central ID: PMC11972613]. https://doi.org/10.1038/s41591-020-0968-3.
5. Wu HJ. Methotrexate works remotely, from the gut. *Cell Host Microbe*. 2021;**29**(3):325-6. [PubMed ID: 33705703]. https://doi.org/10.1016/j.chom.2021.02.016.
6. Yuan Y, Cao D, Zhang Y, Ma J, Qi J, Wang Q, et al. Cryo-EM structures of MERS-CoV and SARS-CoV spike glycoproteins reveal the dynamic receptor binding domains. *Nat Commun*. 2017;**8**:15092. [PubMed ID: 28393837]. [PubMed Central ID: PMC5394239]. https://doi.org/10.1038/ncomms15092.
7. Khan SA, Zia K, Ashraf S, Uddin R, Ul-Haq Z. Identification of chymotrypsin-like protease inhibitors of SARS-CoV-2 via integrated computational approach. *J Biomol Struct Dyn*. 2021;**39**(7):2607-16. [PubMed ID: 32238094]. https://doi.org/10.1080/07391102.2020.1751298.
8. Wu C, Liu Y, Yang Y, Zhang P, Zhong W, Wang Y, et al. Analysis of therapeutic targets for SARS-CoV-2 and discovery of potential drugs by computational methods. *Acta Pharm Sin B*. 2020;**10**(5):766-88. [PubMed ID: 32292689]. [PubMed Central ID: PMC7102550]. https://doi.org/10.1016/j.apsb.2020.02.008.
9. Goyal B, Goyal D. Targeting the Dimerization of the Main Protease of Coronaviruses: A Potential Broad-Spectrum Therapeutic Strategy. *ACS Comb Sci*. 2020;**22**(6):297-305. [PubMed ID: 32402186]. https://doi.org/10.1021/acscombsci.0c00058.
10. Kumar S, Kaushik N. Metabolites of endophytic fungi as novel source of biofungicide: a review. *Phytochemistry Reviews*. 2013;**11**(4):507-22. https://doi.org/10.1007/s11101-013-9271-y.
11. Yasuhara-Bell J, Lu Y. Marine compounds and their antiviral activities. *Antiviral Res*. 2010;**86**(3):231-40. [PubMed ID: 20338196]. [PubMed Central ID: PMC7132374]. https://doi.org/10.1016/j.antiviral.2010.03.009.
12. Zarei A, Ramazani A, Pourmand S, Sattari A, Rezaei A, Moradi S. In silico evaluation of COVID-19 main protease interactions with honeybee natural products for discovery of high potential antiviral compounds. *Nat Prod Res*. 2022;**36**(16):4254-60. [PubMed ID: 34498974]. https://doi.org/10.1080/14786419.2021.1974435.
13. Mohammad-Rezaei R, Khalilzadeh B, Rahimi F, Moradi S, Shahlaei M, Derakhshankhah H, et al. Simultaneous removal of cationic and anionic dyes from simulated industrial effluents using a nature-inspired adsorbent. *Environ Res*. 2022;**214**(Pt 3):113966. [PubMed ID: 35952738]. https://doi.org/10.1016/j.envres.2022.113966.
14. Moradi S, Khani S, Ansari M, Shahlaei M. Atomistic details on the mechanism of organophosphates resistance in insects: Insights from homology modeling, docking and molecular dynamic simulation. *Journal of Molecular Liquids*. 2019;**276**:59-66. https://doi.org/10.1016/j.molliq.2018.11.152.
15. Carroll AR, Copp BR, Davis RA, Keyzers RA, Prinsep MR. Marine natural products. *Nat Prod Rep*. 2021;**38**(2):362-413. [PubMed ID: 33570537]. https://doi.org/10.1039/d0np00089b.
16. Blunt JW, Copp BR, Munro MH, Northcote PT, Prinsep MR. Marine natural products. *Nat Prod Rep*. 2005;**22**(1):15-61. [PubMed ID: 15692616]. https://doi.org/10.1039/b415080p.
17. Kuntz ID, Blaney JM, Oatley SJ, Langridge R, Ferrin TE. A geometric approach to macromolecule-ligand interactions. *J Mol Biol*. 1982;**161**(2):269-88. [PubMed ID: 7154081]. https://doi.org/10.1016/0022-2836(82)90153-x.
18. Sobolev V, Wade RC, Vriend G, Edelman M. Molecular docking using surface complementarity. *Proteins: Structure, Function, and Genetics*. 1996;**25**(1):120-9. https://doi.org/10.1002/(sici)1097-0134(199605)25:1<120::Aid-prot10>3.3.Co;2-1.
19. Kutzner C, Pall S, Fechner M, Esztermann A, de Groot BL, Grubmuller H. More bang for your buck: Improved use of GPU nodes for GROMACS 2018. *J Comput Chem*. 2019;**40**(27):2418-31. [PubMed ID: 31260119]. https://doi.org/10.1002/jcc.26011.
20. Panzade S. *Molecular Dynamics Simulations of Flaviviridae Family fusion peptides*. 2015.
21. Hirshman SP, Whitson JC. Steepest-descent moment method for three-dimensional magnetohydrodynamic equilibria. *The Physics of*

Fluids. 1983;**26**(12):3553-68. https://doi.org/10.1063/1.864116.

22. Nyporko AY. COMPARATIVE STUDY OF PROTEIN MOLECULAR DYNAMICS TRAJECTORIES OBTAINED WITH DIFFERENT COMPU-TATIONAL PARAMETERS. *THE SEVENTH*. 2010:204.
23. Martonak R, Laio A, Parrinello M. Predicting crystal structures: the Parrinello-Rahman method revisited. *Phys Rev Lett*. 2003;**90**(7):75503. [PubMed ID: 12633242]. https://doi.org/10.1103/PhysRevLett.90.075503.
24. Hess B, Bekker H, Berendsen HJ, Fraaije JG. LINCS: A linear constraint solver for molecular simulations. *Journal of Computational Chemistry*. 1997;**18**(12):1463-72. https://doi.org/10.1002/(sici)1096-987x(199709)18:12<1463::Aid-jcc4>3.0.Co;2-h.
25. Van Gunsteren WF, Berendsen HJC. A Leap-frog Algorithm for Stochastic Dynamics. *Molecular Simulation*. 2007;**1**(3):173-85. https://doi.org/10.1080/08927028808080941.
26. Laskowski RA, Swindells MB. LigPlot+: multiple ligand-protein interaction diagrams for drug discovery. *J Chem Inf Model*. 2011;**51**(10):2778-86. [PubMed ID: 21919503]. https://doi.org/10.1021/ci200227u.